

RSC Advances



This is an *Accepted Manuscript*, which has been through the Royal Society of Chemistry peer review process and has been accepted for publication.

Accepted Manuscripts are published online shortly after acceptance, before technical editing, formatting and proof reading. Using this free service, authors can make their results available to the community, in citable form, before we publish the edited article. This *Accepted Manuscript* will be replaced by the edited, formatted and paginated article as soon as this is available.

You can find more information about *Accepted Manuscripts* in the [Information for Authors](#).

Please note that technical editing may introduce minor changes to the text and/or graphics, which may alter content. The journal's standard [Terms & Conditions](#) and the [Ethical guidelines](#) still apply. In no event shall the Royal Society of Chemistry be held responsible for any errors or omissions in this *Accepted Manuscript* or any consequences arising from the use of any information it contains.

pH dependent redox mechanism and evaluation of kinetic and thermodynamic parameters of a novel anthraquinone

Khurshid Ahmad^a, Aamir Hassan Shah^a, Bimalendu Adhikari^b, Usman Ali Rana^c, Syed Noman uddin^a, Chandrika Vijayarathnam^b, Niaz Muhammad^d, Shaukat Shujah^e, Abdur Rauf^f, Hidayat Hussain^f, Amin Badshah^a, Rumana Qureshi^a, Heinz-Bernhard Kraatz^b and Afzal Shah^{*a,b}

^aDepartment of Chemistry, Quaid-i-Azam University, 45320, Islamabad, Pakistan

^bDepartment of Physical and Environmental Sciences, University of Toronto

Scarborough, 1265 Military Trail, Toronto, M1C 1A4, Canada

^cDeanship of scientific research, College of Engineering, King Saud University, Riyadh 11421,

Saudi Arabia

^dDepartment of Chemistry, Abdul Wali Khan University Mardan, Pakistan

^eDepartment of Chemistry, Kohat University of Science & Technology, Kohat, Pakistan

^fDepartment of Biological Sciences and Chemistry, University of Nizwa, 616, Birkat Al Mauz, Nizwa, Oman

*To whom correspondence should be addressed

Tel: 416-208-2776

E-mail: afzal.shah@utoronto.ca

and afzals_qau@yahoo.com

Abstract

The redox behavior of 1,4-dihydroxy-2-(3-hydroxy-3-(trichloromethyl)pentyl)-8-methoxyanthracene-9,10-dione (HCAQ) was investigated at a glassy carbon electrode over a wide pH range of 3-12 by using cyclic, square wave and differential pulse voltammetry (CV, SWV and DPV). Cyclic voltammetric results of HCAQ obtained at different temperatures were used for the evaluation of thermodynamic parameters like ΔG^\ddagger , ΔH^\ddagger and ΔS^\ddagger . The values of diffusion coefficient and heterogeneous electron transfer rate constant were also determined by CV. Limit of detection and quantification was determined by SWV. The number of electrons and protons involved in the oxidation processes were evaluated by DPV. The value of apparent acid dissociation constant (pKa) was obtained from the intersection of two linear segments of the E_p vs pH plot. The effect of pH on the UV-Vis spectral response was also monitored which allowed the determination of pKa of HCAQ. The values of apparent acid dissociation constant obtained from electrochemical techniques and electronic absorption spectroscopy were found in very good agreement. On the basis of experimental results, pH dependent oxidation mechanism was proposed in order to provide useful insights about the unexplored pathways by which AQs exert their biochemical action.

Key words: Rate constant; Redox mechanism; Limit of detection; Thermodynamics of electrode processes; Apparent acid dissociation constant

1. Introduction

Anthraquinones (AQs), an important class of natural evolutionary redox molecules are bestowed with broad range applications.¹ AQs found in some plants and animals are used as constituents of many dyes.²⁻⁴ A number of their derivatives play a key role in catalyzing reduction of biologically important molecules like vitamin K.⁴ Some of the AQs find use as algacides and fungicides.⁵ Their derivatives, being electron acceptor, play a major role in photosynthesis and are able to transport a negative charge in biological systems.⁶ Due to the adsorption ability of AQs at a glassy carbon electrode; their derivatives are used for electrode modification.⁷ The modified electrode can be used as redox catalyst for the reduction of oxygen to hydrogen peroxide.⁸⁻¹⁰ On complexation with macrocyclic polyether, AQs form lumophores that can selectively detect many transition metal ions in solution, thus, offering an alternative photophysical detection mechanism.¹¹ Some AQs like rufigallol and aclarubicin are used as antimalarial¹² and anticancer drugs.¹³ AQs, being redox catalysts, play a vital role in the production of paper pulp.^{14, 15} Alizarin, a derivative of AQ, is extensively used in laboratory as pH indicator, indicator of bone growth and spot test reagent^{16, 17} due to its color variation in different pH media. Apart from pH dependent photophysical properties, the voltammetric behavior of anthraquinones also depends on pH and their potential–pH diagrams can give useful information about the stability of different forms of AQs in acidic, basic and neutral conditions.¹⁸ AQs can be used for electrochemical switchable devices and pH responsive drug delivery systems on the basis of strong pH dependency of their redox behavior.¹⁹⁻²³ The broad range of applications of such compounds prompted us to investigate the electrochemical behavior of a novel anthraquinone, 1,4-dihydroxy-2-(3-hydroxy-3-(trichloromethyl)pentyl)-8-methoxyanthracene-9,10-dione (HCAQ) in a wide pH range. The current work will assist in

explaining some of the redox properties of AQs which are still unexplored by the scientific community. Although extensive literature is available about the voltammetric reduction of AQs, yet, information about their electro-oxidation is meager and investigation of pH dependent oxidation of AQs at different temperature values is an unexplored matter. So to bridge this gap, pH dependent electro-oxidation of HCAQ was investigated at different temperatures with the objectives of adding a new candidate to the literature of AQ family and providing useful insights about the pH dependent electrochemical fate of AQs.

Anthraquinones are commonly used as electron transfer mediators and redox probes.²⁴ Feng and coworkers demonstrated the enhancement in power output of microbial fuel cell by the mediator role of an AQ derivative for efficiently transferring the electron from bacteria to the anode.²⁵ The results of Kumamoto *et al* reveals that oligonucleotide modified with AQ can act as a suitable redox reporter for the detection of a single-base mismatch in DNA.²⁶ Ferapontova and coworker also used AQ as redox probe for the investigation of the electron transfer mechanism within loosely compact monolayers of DNA.²⁷ Most of the AQs exhibit redox behavior in the negative potential domain of glassy carbon or gold electrode but interestingly our anthraquinone derivative, HCAQ can also show redox response in the positive potential window of the electrode. Hence, in comparison to simple AQ, it has extended applications as redox probe and electron transfer mediator.

The biological activities of AQs are related to their redox reactions.^{28, 29} The biological activity of hydroxy quinones is considered to correspond with its hydroxyl group.^{30, 31} Therefore, the presence of three hydroxy functionalities in HCAQ is expected to have broader spectrum of biological activities as compared to simple anthraquinone or its derivatives having single or double hydroxyl groups. By bringing modification in the position of hydroxyl group,

the redox properties of the quinonoid moiety can be altered.³² Thus, more alteration in the properties of HCAQ is possible due to the possibility of changing the position of several hydroxyl groups in its structure.

2. Experimental

Analytical grade reagent, 1,4-dihydroxy-2-(3-H-3-(trichloromethyl)pent)-8-methoxyanth 9,10-dione (HCAQ) was gifted by Prof. Dr. Amin Badshah. A 2 mM stock solution of HCAQ was prepared in absolute ethanol. Fresh working solutions of HCAQ were prepared in 50% ethanol and 50% buffer. Britton-Robinson (BR) buffer of 0.2 M ionic strength with pH 3-12.0 was used as supporting electrolyte. For the preparation of BR buffer, a 0.04 M mixture of each the H_3BO_3 , H_3PO_4 and CH_3COOH was used and adjusted to the desired pH with 0.2 M NaOH.³³

The solution of the analyte was purged with nitrogen gas before every voltammetric assay to remove the dissolved oxygen. All voltammetric experiments were performed using Autolab running with GPES 4.9 software, Eco-Chemie, The Netherlands. A glassy carbon (GC) having surface area of 0.071 cm^2 was used as the working electrode. Pt wire and Ag/AgCl (3 M KCl) were used as counter and reference electrodes. The GCE was polished before each experiment with diamond spray of $1 \mu\text{m}$ particle size. After polishing, the electrode was thoroughly rinsed with a jet of doubly distilled water. The clean electrode was then placed in the desired buffer electrolyte and various differential pulse voltammograms (DPVs) were recorded until the achievement of a steady state base line voltammogram. This procedure ensured reproducible experimental results. The measurement cell was immersed in a water circulating bath (IRMECO I-2400 GmbH Germany) in order to control the temperature. The experimental

conditions for DPV were pulse amplitude 50 mV and pulse width 70 ms. For square wave voltammetry (SWV), the experimental conditions were 50 Hz frequency and 2 mV potential increments corresponding to an effective scan rate of 100 mVs⁻¹. Absorption spectra were recorded on Shimadzu 1601 spectrophotometer and for pH measurements INOLAB pH meter with Model no pH 720 was used.

3. Results and discussion

3.1 Cyclic voltammetry

To obtain a general picture of the redox behavior of the compound, cyclic voltammograms of HCAQ were recorded in different pH media using a potential window of ± 1.3 V. The voltammograms obtained in pH 3.0 and 7.0 can be seen in **Fig. 1**. The CV response under neutral conditions (pH = 7) depicts a sharp oxidation signal, 1a, at +0.69 V, followed by a broad peak, 2a, at +1.02 V. The absence of reduction peak corresponding to 1a and 2a in the backward scan at pH 7.0 demonstrates the irreversible nature of these electrochemical oxidation processes. The compound shows two successive one electron reductions in the negative potential domain of GCE. The reduced species as a result of peaks 1c and 2c gets re-oxidized at nearly the same potential as evidenced by a single broad oxidation peak, 2a*. For confirming 2a* to be the combination of two overlapping peaks, a more sensitive electrochemical technique, differential pulse voltammetry was employed. The differential pulse voltammograms of the analyte shown in **Fig. S-1** unequivocally represents the splitting of peak 2a* into two sub peaks at lower concentration. The anodic and cathodic peak potential differences witness the first and second reductions to follow reversible and quasi-reversible processes. Unlike the behavior of the analyte

in pH 7.0, the backward CV scan in pH 3.0 shows an oxidation dependent reduction peak at +0.33 V. The different voltammetric signature in acidic and neutral media indicates the redox behavior HCAQ to depend strongly on the pH of the medium.

The experiment based on the variation of peak current, I_p , with scan rate, v , was used for the determination of diffusion coefficient and heterogeneous electron transfer rate constant. The scan rate effect of HCAQ was monitored in pH 7.0 at different temperatures. The voltammograms at 323 K shown in **Fig. 2A** demonstrates a linear increase in I_p with the square root of scan rate. Peak 1a shows a large potential shift with scan rate while the reduction peaks exhibit a slight shift in potential. These voltammetric features are characteristics of irreversible (peak 1a) and quasi-reversible redox processes (peak 2c). The values of diffusion coefficients at different temperatures were obtained from the plots of I_p (current intensity of peak 1a) *versus* square root of scan rate (**Fig.3**) using Randles–Sevcik equation.³⁴

$$I_p = \frac{5.16 \times 10^6 n (\alpha_a n)^{1/2} A C D^{1/2} v^{1/2}}{T^{1/2}} \quad 3.1$$

where n is the number of electrons transferred, α_a is the anodic charge transfer coefficient, A , D , C and v are the area of the electrode in cm^2 , diffusion coefficient in $\text{cm}^2 \text{s}^{-1}$, bulk concentration of the species in mol cm^{-3} and scan rate in Vs^{-1} respectively. The values of $\alpha_a n$ using $E_p - E_{p/2} = \frac{0.0477}{\alpha_a n}$ were determined for irreversible process at different temperatures ranging from 308 – 328 K. An examination of **Fig. 2B** reflects that the effect of temperature on peak potential of irreversible process is more pronounced as compared to quasi-reversible process due to their respective kinetic and thermodynamic controlled nature. The values of D at different temperature show an increasing trend with rise in temperature due to the probable decrease in viscosity of the

media. The slope values of $\log I_p$ vs. $\log v$ fall in the range of 0.50–0.53 at all temperatures, thus, indicating the redox process to be limited by diffusion.³⁵

Heterogeneous rate constant (k_s) is an important diagnostic criterion for predicting the nature of redox process. Large values of k_s suggest that following the application of an applied potential, equilibrium between the oxidized and reduced species gets re-established quickly. While small values of k_s indicate slow kinetics and longer time requirement for equilibrium.^{36, 37} The values of k_s listed in **Table 1** were calculated on the basis of peak 1a (**Fig 1**) at different temperatures using equation 3.2.^{38, 39}

$$I_p = nFAk_sC \quad 3.2$$

Where n , F , A and k_s are number of electrons, Faraday's constant, area of the electrode and heterogeneous electron transfer rate constant.

The heterogeneous electron transfer rate constant of HCAQ was evaluated from the peaks corresponding to quasi-reversible redox process using the following form of Nicholson equation.⁴⁰

$$k_s = \Psi \sqrt{\pi D_o a v} \quad 3.3$$

where Ψ is charge transfer parameter, D_o the diffusion coefficient of the oxidized species, v the scan rate and $a = nF/RT$. The values of dimensionless parameter, Ψ , were determined from the difference of anodic and cathodic peak potential difference.⁴¹ The tabulated k_s values (**Table 2**) of a quasi-reversible redox process of HCAQ are greater than irreversible oxidation as expected.⁴² The values of ΔE_p at the experimental temperatures were converted to ΔE_p^{298} by using equation 3.4.⁴³

$$\Delta E_p^{298} = \left(\frac{298}{T} \right) [\Delta E_p^T] \quad 3.4$$

The k_s values (listed in **Table 1**) corresponding to redox process labelled as 1a was used for the determination of thermodynamic parameters. ΔG^\ddagger was evaluated by equation 3.5.⁴⁴

$$\Delta G^\ddagger = 5778.8(5.096 - \log k_s) \quad 3.5$$

With increase in temperature, heterogeneous rate constant increases and ΔG^\ddagger gets lowered. The Arrhenius equation $k_s = Ae^{-\frac{E_a}{RT}}$ was used for the calculation of enthalpy and entropy changes of activation. E_a obtained from the slope of plot of $\log k_s$ against $1/T$ (**Fig. 4**) allowed the evaluation of ΔH^\ddagger and ΔS^\ddagger according to eq. 3.6 and 3.7. An examination of **Table 3** reveals increase in ΔS^\ddagger and a slight decrease in ΔH^\ddagger values with rise in temperature.

$$\Delta H^\ddagger = E_a - RT \quad 3.6$$

$$\Delta G^\ddagger = \Delta H^\ddagger - T\Delta S^\ddagger \quad 3.7$$

The positive ΔH^\ddagger value is responsible for the non-spontaneity of the oxidation reaction. The slight decrease in ΔH^\ddagger with temperature elevation shows the tendency of the electrode process towards spontaneity. The trend of ΔS^\ddagger shown in **Table 3** indicates that at high temperature, the oxidized product of HCAQ diffuses quickly from the electrode surface towards the solution. The trend is the same as predicted by transition state theory $\left[k = \kappa \frac{k_B T}{h} e^{-\frac{\Delta H^\ddagger}{RT}} e^{\frac{\Delta S^\ddagger}{R}} \right]$ ⁴⁵ thus, at higher temperature the increase in ΔS^\ddagger and decrease in ΔH^\ddagger are responsible for higher rate constant values.

3.2. Differential pulse voltammetry

Differential pulse voltammetric technique is associated with the ability of minimizing charging current and consequent enhanced sensitivity.⁴⁶ Therefore, the redox behavior of HCAQ was

investigated by DPV in media of different pH. The DPVs shown in **Figs. 5A** and **S-2** indicates the shift in peak potentials with changing pH. This behavior corresponds to the involvement of protons during electron transfer processes. Moreover, the shift of E_{pa} towards lower potentials with increasing pH shows facile electron abstraction under basic conditions. The differential pulse voltammograms in the potential domain of 0 to +1.3 V show two oxidation peaks in low pH and three in high pH conditions. The DPV was also employed to study the reduction of HCAQ. The potential scan in the negative going direction depicts a couple of peaks corresponding to the two step reduction of HCAQ. The DPV in the potential domain of -1.3 to 0 V followed after scanning from 0 to -1.3 V without cleaning the electrode surface shows a single reverse oxidation peak. Peak 1a with a width at half peak height ($W_{1/2}$) of 54 mV indicates the involvement of two electrons in this oxidation step.⁴⁷ For the determination of the number of protons involved in oxidation process, peak potential was plotted against pH.

The slope of the plot shown in **Figs. 5B** shows the oxidation (corresponding to peak 1a) to occur by the involvement of two protons and two electrons. The intersection of the two linear segments of E_p vs pH plots indicates HCAQ to have apparent acid dissociation constant value of 10.4. In contrast to 1a, peak 2a is broad indicating one electron loss during this oxidation step. The plot of peak potential *versus* pH shown in **Fig S-3** demonstrates the removal of an electron to be accompanied by a proton. Similar behavior was also observed for peak 2a'.

3.3. Square wave Voltammetry

Square wave voltammetry (SWV) being one of the most sensitive and fast electrochemical techniques⁴⁸ was employed to determine the limit of detection (LOD) and limit of quantification (LOQ) of HCAQ. From the calibration curves (**Fig. S-4A**), LOD and LOQ with values 0.08 and 0.26 mmolL⁻¹ were determined according to the reported equation 3.8 and 3.9.⁴⁹

$$\text{LOD} = \frac{3S}{m} \quad 3.8$$

$$\text{LOQ} = \frac{10S}{m} \quad 3.9$$

where S is standard deviation of the intercept and m the slope of the plot of peak current *versus* concentration shown in **Fig. S-4B**.

3.4. Electronic absorption spectroscopy

UV-Vis spectroscopy was carried out for the purpose of photometric characterization and confirmation of the apparent acid dissociation constant obtained from electrochemical techniques. Simple anthracenedione has been reported to give four electronic absorption signals.⁵⁰ The signal at 207 nm is attributed to $n - \sigma^*$ transition of carbonyl group while the others are assigned to $\pi - \pi^*$ transition. The signal at 252 nm is allocated to $\pi - \pi^*$ transition of benzenoid system and those at 272 and 326 nm are assigned to $\pi - \pi^*$ transition of quinonoid system. The assignment of signals is made on the basis of comparison with UV spectrum of anthracene.⁵⁰ The UV-visible spectra of HCAQ show five signals (**Fig.6A**). The signal at 207 nm ($n - \sigma^*$ transition of carbonyl group) is absent in the spectrum of HCAQ due to blocking of lone pair on C = O because of possible hydrogen bonding between OH at 1 and 4 positions. The signals at 232 and 252 nm are assigned to $\pi - \pi^*$ transitions of benzenoid system while that at 287 nm is assigned to $\pi - \pi^*$ transition of quinonoid system.^{50,51} The splitting of benzenoid band may be due to the existence of mesomeric structures or conjugation breakage. The broad band (at 425-550 nm) lacking in the absorption spectrum of simple anthraquinone⁵² is present in the spectrum of HCAQ. As hydroxyl group is electron donating and gives absorption band in the visible region by charge transfer (CT) mechanism^{51, 53} so the spectral band displacements are

related to the increase in length of chromophore by additional rings formation due to intermolecular hydrogen bonding.^{53, 54}

The absorption spectra of HCAQ in different pH media are shown in **Fig. 6B**. An observation of the spectra reveals that the absorption band due to CT mechanism is strongly affected by the pH as compared to other peaks. The band corresponding to CT mechanism of the orange colored solution appears in the range of 470-500 nm at $\text{pH} < 9$ and gets shifted to 552-590 nm at $\text{pH} \geq 9$ due to deprotonation of HCAQ. The drastic color variation (see **Fig. 7**) of HCAQ from pH 10 to 11 unequivocally indicates HCAQ to ionize at $\text{pH} \sim 10$. The isosbestic point at 299 nm denotes HCAQ and its mesomeric form to exist in equilibrium with the same value of molar extinction coefficient. The presence of OH group at positions 1 and 4 are responsible for the mesomeric form of HCAQ. Another isosbestic point at 516 nm represents HCAQ and its deprotonated form to exist in equilibrium and absorb the same amount of light at this wavelength. Isosbestic point typically indicates the presence of only two species.⁵⁵⁻⁵⁷ The occurrence of isosbestic points in multicomponent solutions is almost impossible because the identical absorbance of three or more compounds at any wavelength is negligibly small.⁵⁵

From the slopes of the plots of absorbance *versus* concentration, the molar extinction coefficients with values shown in **Fig. 8A** were calculated at respective wavelengths. On the basis of the peaks at 475 and 554 nm, the apparent acid dissociation constant of HCAQ with a value of 10.1 was obtained from the plot of absorbance *versus* pH as shown in **Fig. 8B**. This apparent acid dissociation constant value is close agreement to that obtained from DPV and drastic color variation of **Fig. 7**.

3.5. Redox Mechanism

The oxidation of HCAQ exhibited two peaks in acidic and three in basic media (see **Fig. 5**). The oxidation corresponding to peak 1a was found to occur by the transfer of two electrons as determined from the average $W_{1/2}$ value of 54 mV. E_{pa} vs. pH plot indicated the oxidation to occur by the involvement of two protons. On the basis of the results obtained from DPV and SWV it is proposed that the hydroxyl groups of HCAQ, after the loss of two electrons and two protons, presumably result in the formation of oxygen radicals³⁸ that may get converted to 2-(3-hydroxy-3-(trichloromethyl)pentyl)-8-methoxyanthracene-1,4,9,10(4aH,9aH)-tetraone⁵⁸ as shown in **Scheme 1**.

Fig. 5 shows that peak 2a is pH dependent in acidic conditions while independent in basic media and thus the mechanistic pathway gets switched from an EC to a CE mechanism (see **Schemes 2A and B**). The average $W_{1/2}$ value and slope of E_{pa} vs. pH plot of peak 2a shows one electron and one proton oxidation process. This peak is assigned to hydroxyl group of pentyl substituent because the trichloromethyl is electron withdrawing group, therefore this hydroxyl group is oxidized at high potential. The DPVs in basic media show the appearance of a third pH dependent peak 2a'. The half peak potential value and shifting of peak position with pH shows the involvement of one electron and one proton in this process. On the basis of these results, a CEC mechanism is proposed as shown in **Scheme 3**. The results of peak width at half peak current and E_{pc} versus pH plots revealed the two steps reduction of HCAQ to occur by the involvement of $1e^-$ and $1H^+$ in each step. The mechanism proposed is shown in **Scheme 4**.

3.6. Conclusion

The compound HACQ was found to oxidize in a pH dependent irreversible manner. The irreversibility of oxidation was ensured by the absence of corresponding reduction peak in the cyclic voltammetric response and the value of rate constant. The effect of temperature was studied for the evaluation of various kinetic and thermodynamic parameters of the compound. The temperature dependent peak shift was found more pronounced on irreversible process as compared to reversible process. Thermodynamic parameters revealed the endothermic nature of the redox processes. Increase in electron transfer rate constant showed the trend of redox process towards reversibility at higher temperature values. The positive enthalpy change showed the redox behavior to be of endothermic nature. Decreased values of Gibbs free energy with increase in temperature indicated the redox processes to become facile at elevated temperature. The pH dependent results of three electroanalytical techniques helped in proposing the redox mechanism of the compound. The electronic absorption spectroscopy showed the charge transfer mechanism to depend strongly on the pH of the medium. The values of apparent acid dissociation constant determined by electronic absorption spectroscopy, DPV and drastic change in solution color were found in very good agreement.

Acknowledgements

The authors gratefully acknowledge the financial support of Higher Education Commission of Pakistan through project number 3070, Quaid-i-Azam University, the University of Toronto Scarborough, NSERC and Deanship of Scientific Research at King Saud University through the research group project number RGP-VPP-345.

References

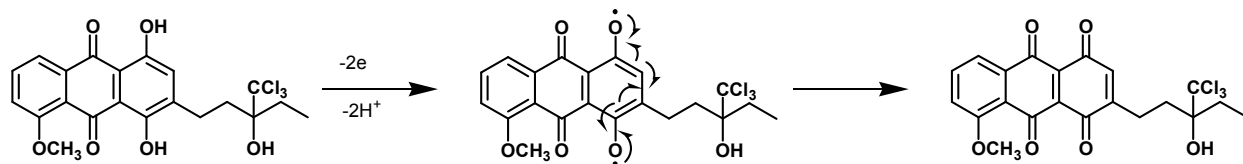
1. W. Ma and Y.T. Long, *Chemical Society Reviews*, 2014, **43**, 30-41.
2. H. Dave and L. Ledwani, *Indian Journal of Natural Products and Resources*, 2012, **3**, 291-319.
3. P. Hietala, M. Marvola, T. Parviainen and H. Lainonen, *Pharmacology & toxicology*, 1987, **61**, 153-156.
4. X. Gong, R. Gutala and A. K. Jaiswal, *Vitamins & Hormones*, 2008, **78**, 85-101.
5. Y.M. Kim, C.H. Lee, H.G. Kim and H.S. Lee, *Journal of agricultural and food chemistry*, 2004, **52**, 6096-6100.
6. H. Görner, *Photochemistry and photobiology*, 2003, **77**, 171-179.
7. A. Salimi, H. Eshghi, H. Sharghi, S. M. Golabi and M. Shamsipur, *Electroanalysis*, 1999, **11**, 114-119.
8. J.M. Campos-Martin, G. Blanco-Brieva and J.L. Fierro, *Angewandte Chemie International Edition*, 2006, **45**, 6962-6984.
9. E. Santacesaria, M. Di Serio, A. Russo, U. Leone and R. Velotti, *Chemical engineering science*, 1999, **54**, 2799-2806.
10. R. Nissim, C. Batchelor-McAuley, Q. Li and R.G. Compton, *Journal of Electroanalytical Chemistry*, 2012, **681**, 44-48.
11. M. Kadarkaraisamy and A. G. Sykes, *Inorganic chemistry*, 2006, **45**, 779-786.
12. R. Winter, K.A. Cornell, L.L. Johnson, M. Ignatushchenko, D.J. Hinrichs and M.K. Riscoe, *Antimicrobial agents and chemotherapy*, 1996, **40**, 1408-1411.
13. A. Koceva-Chyla, M. Jedrzejczak, J. Skierski, K. Kania and Z. Józwiak, *Apoptosis*, 2005, **10**, 1497-1514.
14. R. Francis, S. J. Shin, S. Omori, T. Amidon and T. Blain, *Journal of wood chemistry and technology*, 2006, **26**, 141-152.
15. E. Zhizhina, K. Matveev and V. Russkikh, *Khimiya v Interesakh Ustoichivogo Razvitiya*, 2004, **12**, 47-51.
16. I.T. Shadi, B.Z. Chowdhry, M.J. Snowden and R. Withnall, *Journal of Raman Spectroscopy*, 2004, **35**, 800-807.
17. D. Hoyte, *Journal of anatomy*, 1960, **94**, 432.

18. M.A.B. Hasan-Susan, M. Begum, Y. Takeoka and M. Watanabe, *Journal of Electroanalytical Chemistry*, 2000, **481**, 192-199.
19. S.I. Bailey and I.M. Ritchie, *Electrochimica Acta*, 1985, **30**, 3-12.
20. G. Jurmann, D.J. Schiffrin and K. Tammeveski, *Electrochimica Acta*, 2007, **53**, 390-399.
21. D. Ajloo, B. Yoonesi and A. Soleymanpour, *International Journal of Electrochemical Science*, 2010, **5**, 459-477.
22. S. Riahi, S. Eynollahi and M.R. Ganjali, *International Journal of Electrochemical Science*, 2009, **4**, 1309-1318.
23. M. Shamsipur, A. Siroueinejad, B. Hemmateenejad, A. Abbaspour, H. Sharghi, K. Alizadeh and S. Arshadi, *Journal of Electroanalytical Chemistry*, 2007, **600**, 345-358.
24. S. Takahashi and J.I. Anzai *Materials*, 2013, **6**, 5742-5762.
25. C. Feng, L. Ma, F. Li, H. Mai, X. Lang and S. Fan, *Biosensors and Bioelectronics*, 2010, **25**, 1516-1520.
26. S. Kumamoto, M. Watanabe, N. Kawakami, M. Nakamura and K. Yamana, *Bioconjugate Chemistry*, 2008, **19**, 65-69.
27. A. Abi, E.E. Ferapontova, *Journal of American Chemical Society*, 2012, **134**, 14499-14507.
28. F.C. de Abreu, P.A.L. De Ferraz, and M.O.F. Goulart, *Journal of the Brazilian Chemical Society*, 2002, **13**, 19-35.
29. A. Bartoszek, *Acta Biochimica Polonica*, 2002, **49**, 323-331.
30. N.U. Frigaard, S. Tokita, and K. Matsuura, *Biochimica et Biophysica Acta*, 1999, **1413**, 108-116.
31. N. Watanabe and H.J. Forman, *Archives of Biochemistry and Biophysics*, 2003, **411**, 145-157.
32. M. Aguilar-Martinez, J.A. Bautista-Martinez, N. Macias-Ruvalcaba, I. Gonzalez, E. Tovar, T. Marín del Alizal, O. Collera and G. Cuevas, *Journal of Organic Chemistry*, 2001, **66**, 8349-8363.
33. H.T.S. Britton and R.A. Robinson, *Journal of the Chemical Society*, 1931, 1456-1462.

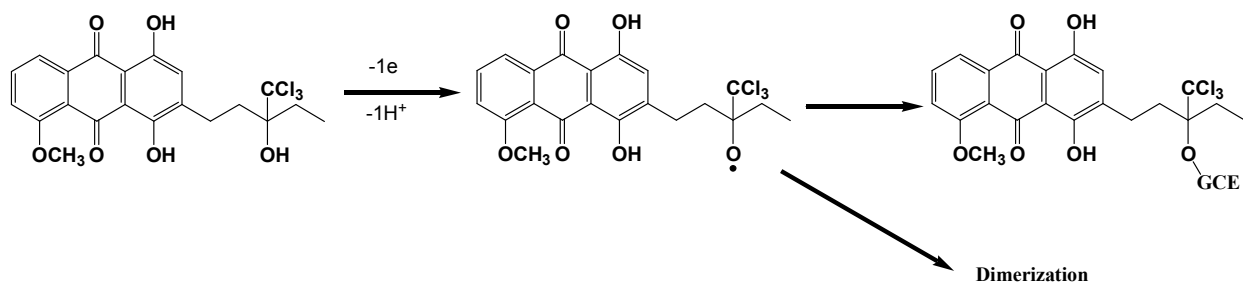
34. J. E. B. Randles, *Transactions of the Faraday Society*, 1948, **44**, 327-338.
35. S.S. Kalanur, J. Seetharamappa, U. Katrahalli and P.B. Kandagal, *Int. J. Electrochem. Sci*, 2008, **3**, 711-720.
36. B.H. McMahon, J.D. Müller, C.A. Wraight and G.U. Nienhaus, *Biophysical journal*, 1998, **74**, 2567-2587.
37. H. Kirchhoff, M.A. Schöttler, J. Maurer and E. Weis, *Biochimica et Biophysica Acta (BBA)-Bioenergetics*, 2004, **1659**, 63-72.
38. S. Munir, A. Shah, A. Rauf, A. Badshah, S.K. Lunsford, H. Hussain and G.S. Khan, *Electrochimica Acta*, 2013, **88**, 858-864.
39. L. Nadjo and J. Savéant, *Journal of Electroanalytical Chemistry and Interfacial Electrochemistry*, 1973, **48**, 113-145.
40. J. Schmitz and J. Van der Linden, *Analytical Chemistry*, 1982, **54**, 1879-1880.
41. R.S. Nicholson, *Analytical Chemistry*, 1965, **37**, 1351-1355.
42. J.J. Zuckerman, *Inorganic Reactions and Methods, Cumulative Index, Part 1: Author and Subject Indexes*, John Wiley & Sons, 2009.
43. P.M.S. Monk, *The viologens: physicochemical properties, synthesis, and applications of the salts of 4,4'-bipyridine*, Wiley, 1998.
44. S.A. Yasin, *Portugaliae Electrochimica Acta*, 2006, **24**, 23-36.
45. K.J. Laidler, *Pure Appl. Chem*, 1981, **53**, 753-771.
46. A.C. Michael and L. Borland, *Electrochemical Methods for Neuroscience*, Taylor & Francis, 2010.
47. T.A. Enache and A.M. Oliveira-Brett, *Journal of Electroanalytical Chemistry*, 2011, **655**, 9-16.
48. S. Altınöz and B. Uyar, *Analytical Methods*, 2013, **5**, 5709-5716.
49. G.D. Christian, *Analytical Chemistry, 6th Ed*, Wiley India Pvt. Limited, 2007.
50. M. El Ezaby, T. Salem, A. Zewail and R. Issa, *Journal of the Chemical Society B: Physical Organic*, 1970, 1293-1296.
51. S.H. Etaiw, M.M. Abou Sekkina, G.B. El-Hefnawey and S.S. Assar, *Canadian Journal of Chemistry*, 1982, **60**, 304-307.
52. Z. Markovic, N. Manojlovic and S. Zlatanovic, *Journal of the Serbian Society for Computational Mechanics*, 2008, **2**, 73-79.

53. A. Navas Diaz, *Journal of Photochemistry and Photobiology A: Chemistry*, 1990, **53**, 141-167.
54. R. N. Capps and M. Vala, *Photochemistry and photobiology*, 1981, **33**, 673-682.
55. M. Sauer, J. Hofkens and J. Enderlein, *Handbook of Fluorescence Spectroscopy and Imaging: From Ensemble to Single Molecules*, Wiley, 2010.
56. S. Doose, H. Neuweiler and M. Sauer, *ChemPhysChem*, 2005, **6**, 2277-2285.
57. T. Heinlein, J.P. Knemeyer, O. Piestert and M. Sauer, *The Journal of Physical Chemistry B*, 2003, **107**, 7957-7964.
58. A. M. Oliveira-Brett, and M. E. Ghica, *Electroanalysis*, 2003, **15**, 1745-1750.

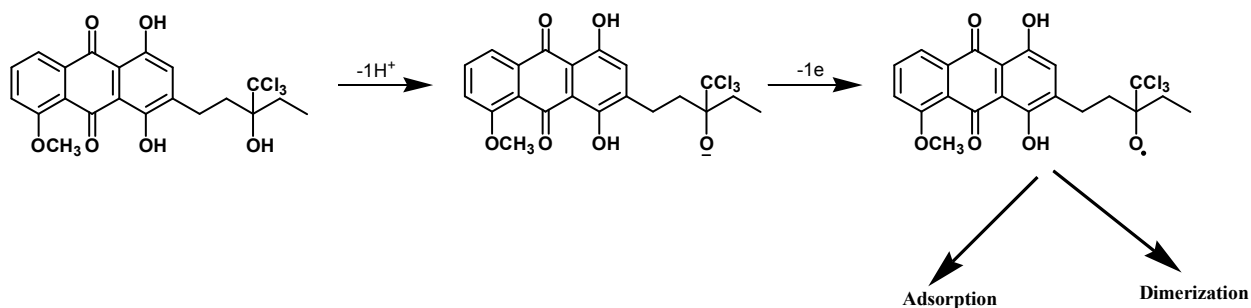
Schemes



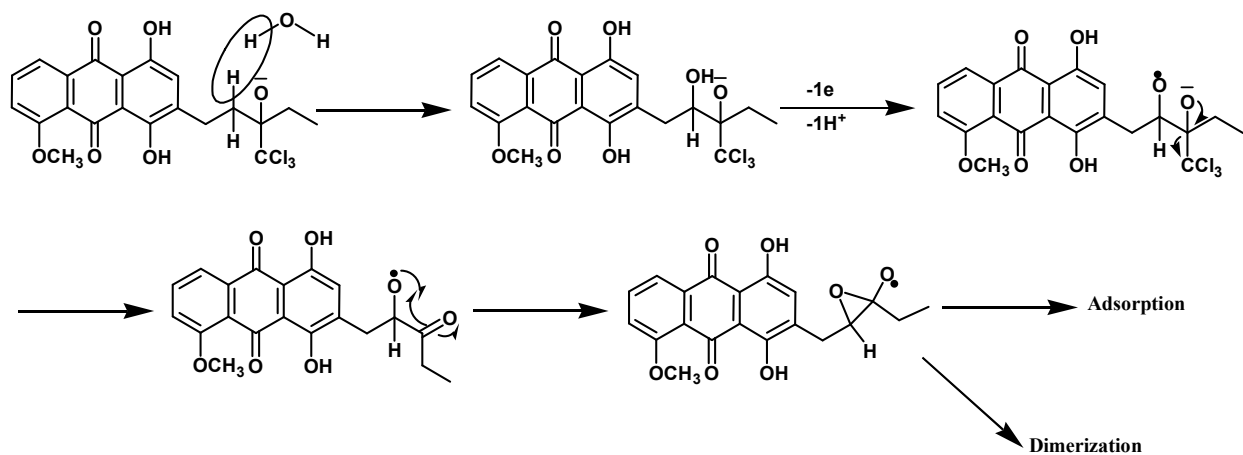
Scheme 1 Proposed oxidation mechanism of HCAQ corresponding to peak 1a.



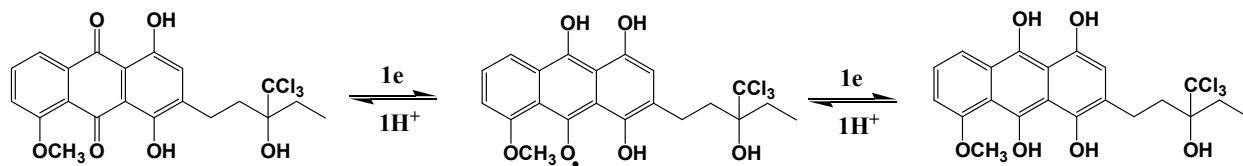
Scheme 2A. Proposed mechanism corresponding to peak 2a showing proton coupled electron loss in acidic conditions.



Scheme 2B. Suggested CE (chemical reaction followed by electron transfer reaction) type oxidation mechanism of HCAQ corresponding to peak 2a in neutral and alkaline conditions.



Scheme 3. Proposed oxidation mechanism of HCAQ corresponding to peak 2a' in neutral and alkaline conditions.



Scheme 4. Proposed redox mechanism of HCAQ corresponding to peaks appearing in the negative potential window of GCE.

Tables

Table 1. Diffusion coefficient and heterogeneous rate constant values of HCAQ evaluated on the basis of oxidation peak 1a at different temperatures.

Peak	Temperature (K)	$1/T \times 10^{-3}$ (K ⁻¹)	αn_a	$D/10^{-7}$ (cm ² s ⁻¹)	$k_s/10^{-4}$ (cm s ⁻¹)	$\log k_s$
1a	308	3.25	0.99	0.16	2.01 (0.02)	3.698
	313	3.19	1.12	0.48	2.31 (0.02)	3.636
	318	3.14	1.25	1.17	3.66 (0.04)	3.437
	323	3.09	1.32	1.34	6.15 (0.07)	3.211
	328	3.05	1.40	4.04	7.27 (0.08)	3.139

Table 2. Heterogeneous electron transfer rate constant values of HCAQ evaluated on the basis of quasi-reversible redox peaks at different temperatures.

Temperature (K)	$k_s / \times 10^{-3}$ (cm s ⁻¹)
313	1.21 (0.04)
318	7.60 (0.19)
323	7.79 (0.16)

Table 3. Thermodynamic parameters of HCAQ

Peak	Temperature (K)	$\Delta G^\#$ /(kJ/mol)	E_a /(kJ/mol)	$\Delta H^\#$ /(kJ/mol)	$\Delta S^\#$ /(J/K.mol)
1a	308	51.00	62.66	60.09	29.54
	313	50.37		60.06	30.95
	318	49.31		60.01	33.67
	323	48.09		59.97	36.77
	328	47.51		59.93	37.87

Although estimated errors in $\Delta G^\#$ and E_a are $\pm 2\%$, additional significant figures are given to allow more accurate calculation of $\Delta H^\#$ and $\Delta S^\#$.

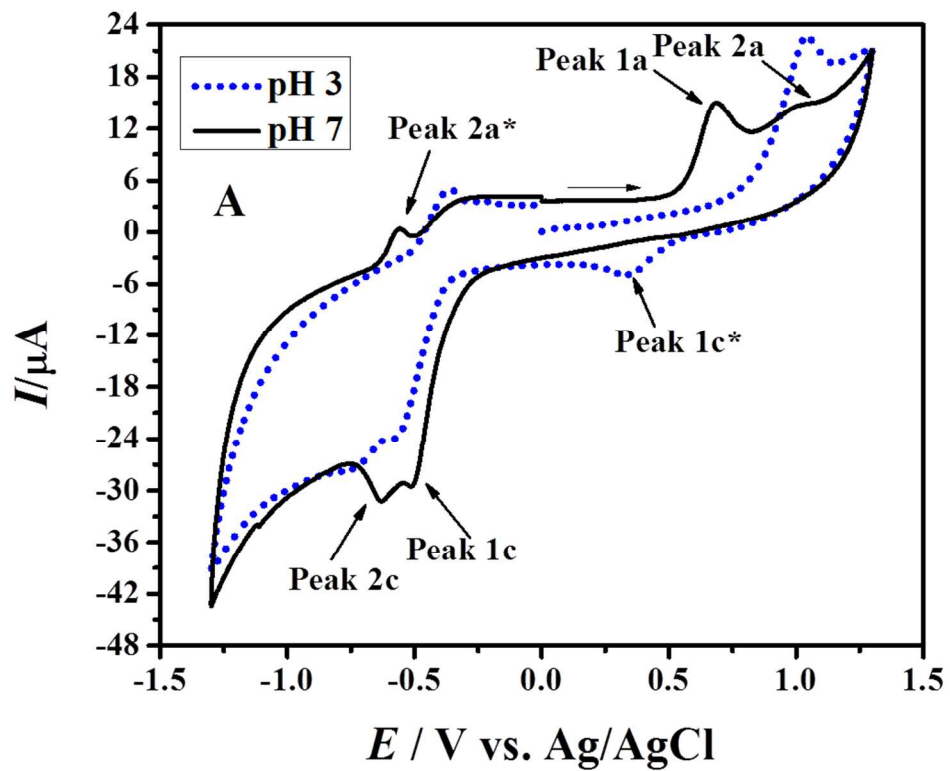


Fig.1. 1st scan CVs of 1 mM HCAQ obtained in pH 3.0 and 7.0 at 100 mVs⁻¹.

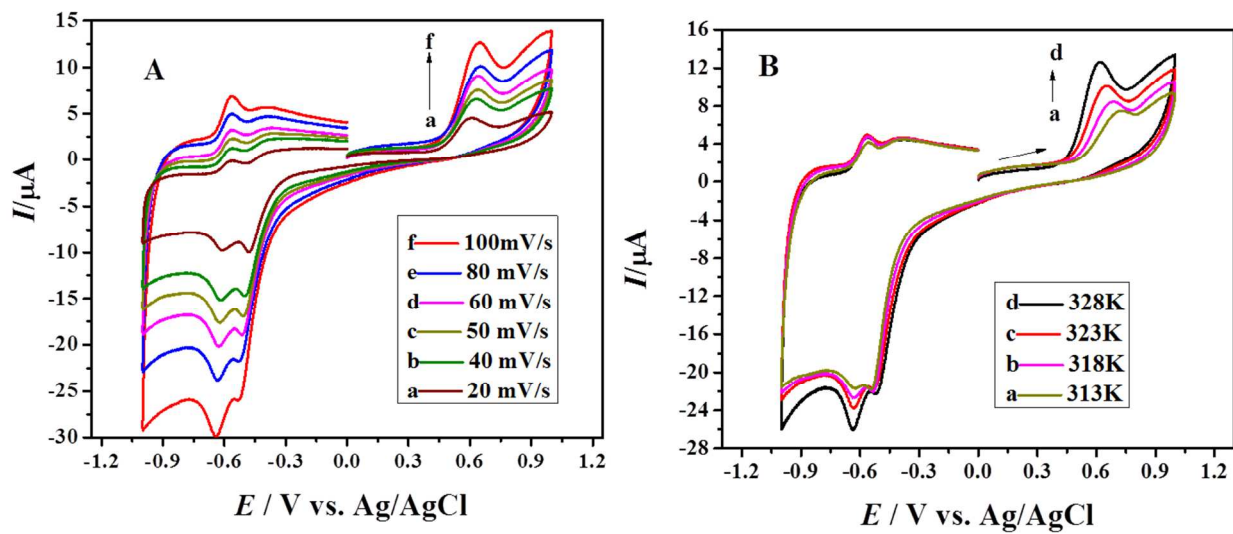


Fig.2. Effect of (A) scan rate at $323 \pm 1\text{K}$ and (B) temperature at 80 mVs^{-1} on the cyclic voltammetric behaviour of 0.7 mM HCAQ.

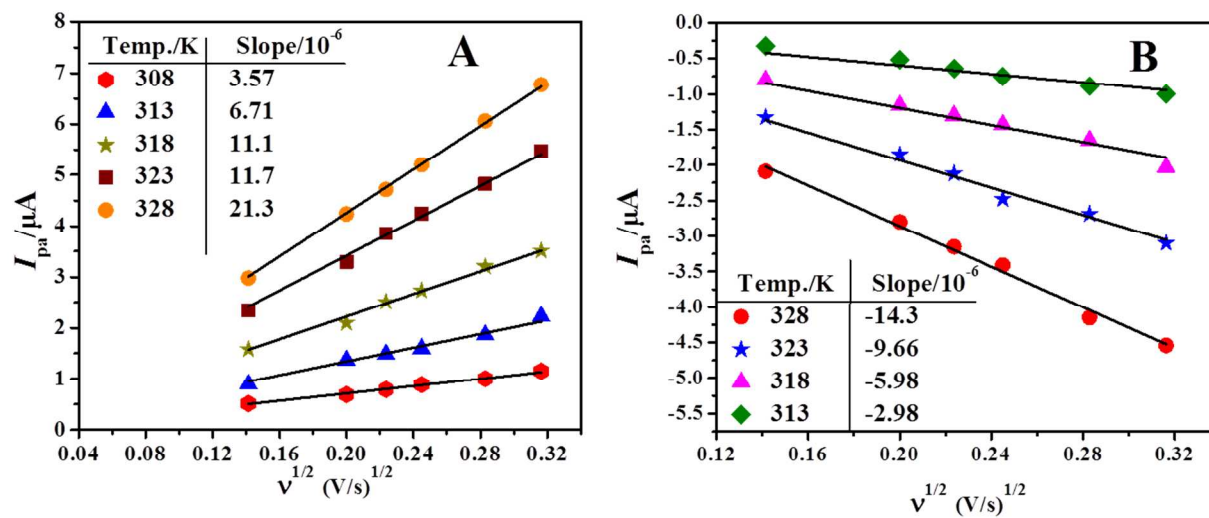


Fig.3. Plots of peak current of (A) 1a and (B) 2c against the square root of scan rate using 0.7 mM solution of HCAQ.

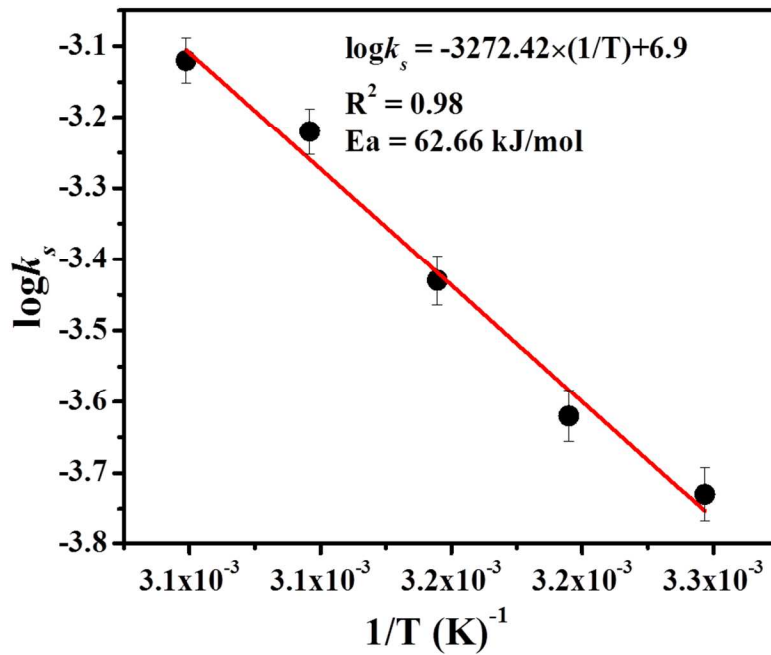


Fig. 4. Plot of $\log k_s$ as a function of $1/T$.

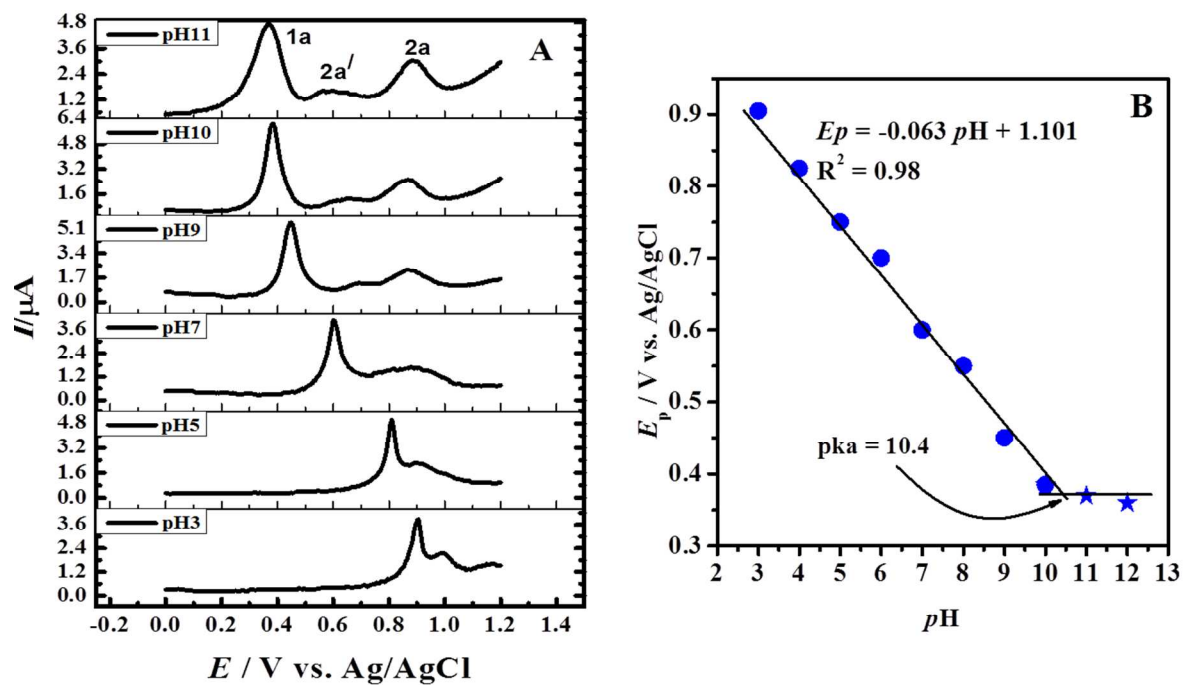


Fig.5. (A) DPVs of 0.7 mM HCAQ recorded at 5 mVs^{-1} in 50% ethanol and 50% BR buffer of pH 3-11(B) Plot of E_p versus pH using DPV data of peak 1a.

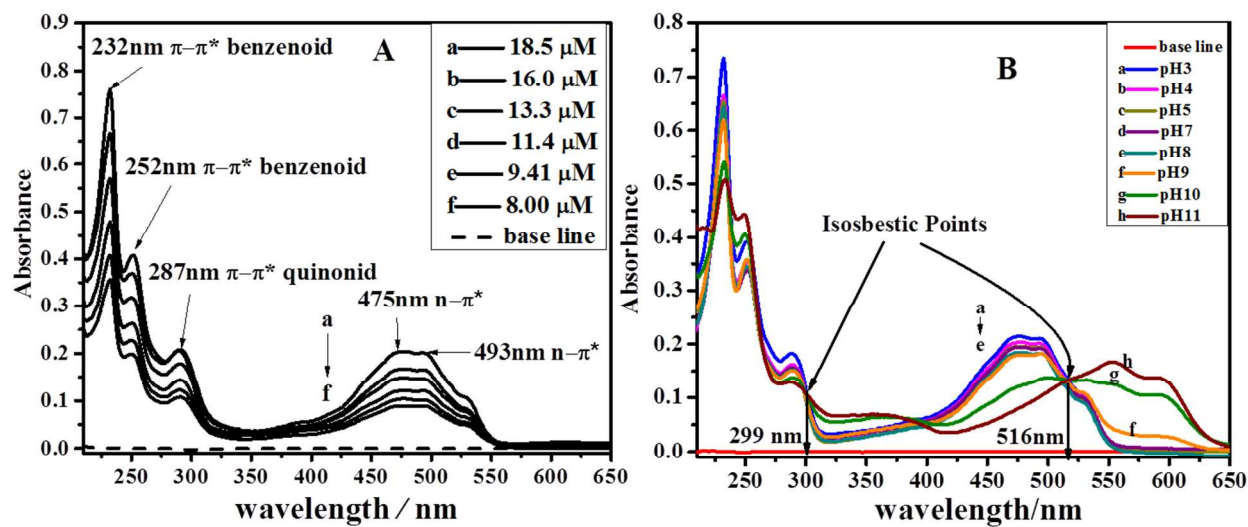


Fig.6. (A) UV-Vis spectra of different concentration of HCAQ obtained in pH 7 (B) Absorption spectra of 16 μM HCAQ recorded in pH 3-11.

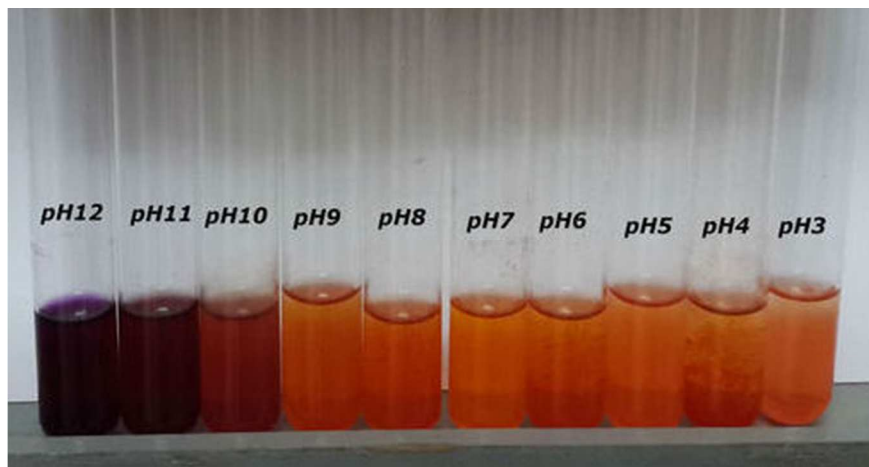


Fig.7. Color variation of 16 μ M HCAQ in pH 3-12.

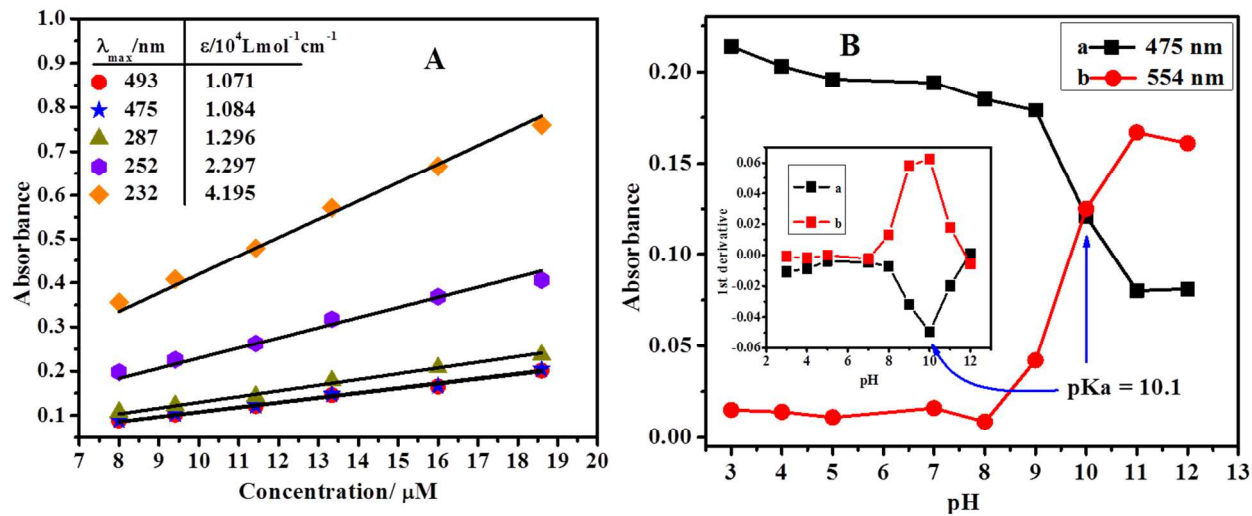


Fig.8. (A) Plots of absorbance *versus* concentration using UV-Vis spectroscopic data obtained in pH 7 (B) Absorbance of 16 μM μM HCAQ as a function of pH.